

B1623

Operation of High Temperature Electrolysis Stacks in the 10-to-20 kW_{DC} range

**Jérôme Aicart, Brigitte Gonzalez, Lucas Champelovier, Amélie Maisse,
Barbara Dhe, Géraldine Palcoux, Stéphane Di Iorio**

Univ. Grenoble Alpes, CEA, Liten, DTCH, 38000 Grenoble, France

Tel.: +33-43878-6744

jerome.aicart@cea.fr

Abstract

The interest in high temperature electrolysis technology is sustained by promises of low cost, low carbon mass hydrogen production. To support the deployment of pre-industrial systems, CEA is devoting significant efforts to scale-up its proprietary stack base design. Partially supported by E.U. project MultiPLHY, this experimental report thus presents galvanostatic and thermoneutral operation of stacks in the 10-to-20 kW_{dc} range.

The laboratory first attempt at manufacturing a larger stack yielded an assembly of three 25-cell substacks [1]. They comprised commercial cathode-supported cells with a 200 cm² active area. After about 700 h of preliminary measurements, the stack was operated for 3.2 kh at -0.65 A.cm⁻², 60% SC and 12.6 kW_{dc} [2], during which a linear evolution of the stack temperature was recorded at a rate of +15 K.kh⁻¹. The overall sequence generated 1.1 ton of H₂, a first in the laboratory history. The end of the test is discussed.

Based on internal advances in design and manufacturing control, a 20 kW_{dc} stack was subsequently manufactured in one go. Moving away from the substack approach allowed reducing the production time by approximately 80%. The stack was then operated in thermoneutral conditions for 5.9 kh at -0.94 A.cm⁻² and 18.6 kW_{dc}, a 50% power boost compared to the first stack. The recorded temperature evolution rate, akin to apparent degradation, had been impressively lower than 1.7 K.kh⁻¹ over 4.8 kh.

In recent years, the standardization of stack tests targeting durations beyond 5 kh [3,4] was enabled by CEA's ability to produce dedicated, purpose-built benches with near-perfect availabilities. Correspondingly, the data of the present work was obtained on a new generation of in-house equipment designed for long-term durability assessments of power-stacks. Bench availability results are discussed.

Introduction

Interest in high temperature electrolysis (HTE) has increased in recent years due to unprecedented efficiencies at (pre-)industrial system level [5] compared to low temperature technologies. Industrialization of HTE is accelerating, and several innovative demonstrators are currently in operation or undergoing their last stages of commissioning: Bloom Energy (4 MW, USA), Sunfire (2.4 MW, DE), Ceres Energy (1 MW, UK), Topsoe (pressurized 0.35 MW, DK). As HTE system power increases, raising the stack power is generally targeted to reduce costs and increase production volumes. In recent years, CEA Liten has devoted significant efforts [6] to upscaling the base design of its proprietary cross-flow stack [1,7–13]. To date, two full-size manufacturing attempts have been made. In this work, these 10-to-20 kW_{DC} power stacks were operated until their respective end-of-life.

1. Experiments

1.1. Stacks Description

The two stacks comprised commercial cathode-supported cells with 196 cm² active areas, with Ni and 8 vol% yttrium-stabilized zirconia (8YSZ) cermet fuel electrodes, 8YSZ electrolytes, Cerium Gadolinium Oxide (CGO) diffusion barriers, and Lanthanum Strontium Cobalt (LSC) oxygen electrodes. In this work, the interconnects were made of AISI441 ferritic stainless steel. Electrical contacts with the electrodes were optimized using Lanthanum Strontium Manganese (LSM) on the air side and Ni meshes on the H₂ side.

The attempt at scaling up the base stack design yielded a pileup of three substacks individually manufactured and conditioned [6,2,1]. Each substack comprised 25 cells. The resulting 3x25-cell stack will be denoted S1 in the following. Based on the knowledge gathered during the manufacturing and testing of S1, S2 was subsequently produced, incorporating slight design modifications. In this case, it consisted in a 78-cell stack assembled and conditioned all at once. This manufacturing success achieved a 25% increase in compactness (less end plates), and a 75% reduction of manufacturing time.

1.2. Stack Operating Strategy

Both stacks were operated in thermoneutral conditions, in order to both maximize the efficiency of the electrochemical conversion and minimize thermal gradients throughout the stacks. As a result, stack temperature evolved over time to compensate degradation and keep the average cell voltage approximately equal to 1.29 V. Due to thermal considerations as well, current ramp rate was set to a high ± 1 (A.cm⁻²).min⁻¹. This overall operating strategy has yielded excellent results in previous works [14,3,15]. Both stacks were operated at 60% SC. At all times, steam inlet was mixed with 10 vol.% H₂ to prevent cermet oxidation.

1.3. Test Bench

A test bench was purpose-designed and built to carry out long-term durability investigations on 10-to-20 kW_{DC} stacks. It is described in Figure 1.

Inlet gas flowrates were controlled using thermal mass flow controllers (Brooks, 5851S and 5853S). A proprietary direct evaporator was used to generate steam from the building ultra-pure deionized water network [15] using a Coriolis flow controller (Brooks, Quantim). Condensation between the steam generator (SG) and the hot zone was prevented using a heating wire. In case of a shutdown of the building power supply, float-flow meters and normally open valves would insure the stack's H₂ compartment is fed with 96/4 vol.% N₂/H₂ and the O₂ compartment with air.

Gas connections to the stack were achieved via a gas connection plate, located at the center of a drop-down furnace (modified Rohde TE 200 S). It comprised three distinct thermal zones individually controlled. The bottom heating element was dedicated to gas preheating using piping loops, as the thermal control strategy was taken from another bench previously developed in the laboratory [4,15]. However, due to the much higher flowrates needed to supply 20 kW stacks, gas/gas nickel-brazed heat exchangers were incorporated to the bench (H050, Kaori). All high temperature piping was made of Inconel 600 and pre-treated to limit Cr evaporation. At the bench outlet, gas exhausts went through a cooling and, in the case of H₂O/H₂, a separation phase. Afterwards, dry flowrates were measured using low pressure drop flowmeters (Whisper, Alicat), before venting in the atmosphere. DC power was generated using a 30 kW reversible supply (PSB 10200-420, EA), and connections to the stacks were achieved using proprietary high temperature conductors. The total electrical consumption of the bench was recorded using a power meter (Diris A40, Socomec).

The stacks inlet and outlet gas temperatures were monitored by inserting type-N thermocouples in the gas connection plate. Similarly, all terminal plates of the stacks were instrumented with four thermocouples, inserted at various depths toward the center of the stacks.

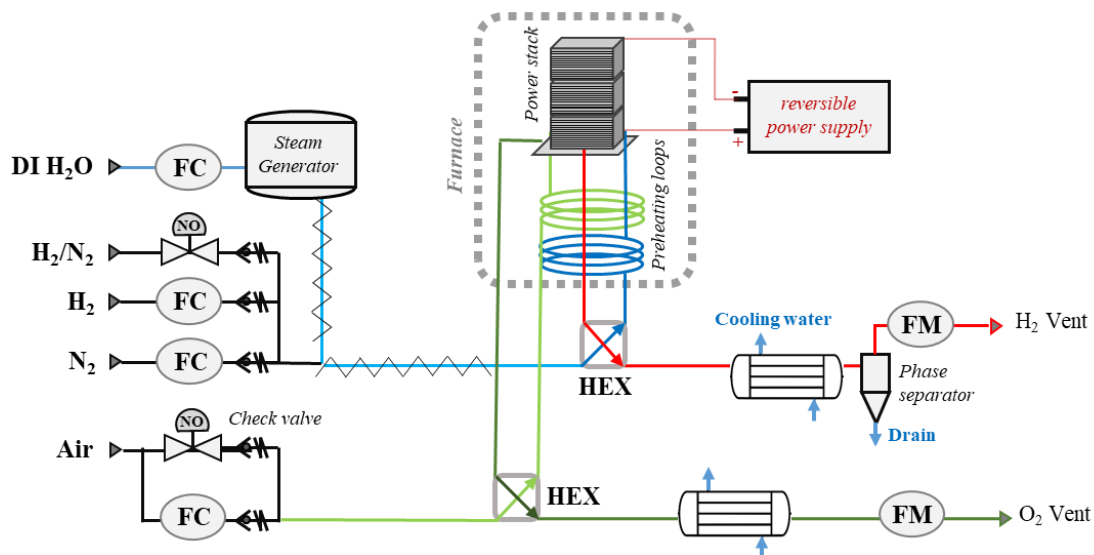


Figure 1: Simplified description of test bench used in this work (FC: flow control, FM: flow measurement, NO: normally open, HEX: heat exchanger).

2. Results & Discussion

2.1. Operation of S1

Figure 2 provides an overview of the first heat-up sequence of S1 following its integration to the durability test bench (Figure 1). From ambient to about 300°C, the ramp rate was about +0.35°C.min⁻¹, a consequence of a self-imposed limitation of keeping the maximum temperature difference between inlet and outlet gases below 25°C. The rest of the temperature ramp was carried out at rates ranging from 0.3 to 0.55°C.min⁻¹. In the context of the test bench, this last value was found to be the quickest rate achievable while maintaining the difference between inlet and outlet gases steady over time. These results are similar to that of a previous work carried out on stacks of comparable size [14], and further suggest that heating homogeneously power stacks as quickly as smaller ones is challenging. While the 30 h ramp time recorded in this work can most probably be optimized, it can be compared to the 4 h objective set by the Clean Hydrogen Partnership for 2030 [16]. Nevertheless, the usefulness of developing future systems capable of achieving such a short cold start time should at the very least be discussed. Indeed, it would require incorporating heating elements of high power that would remain mostly unused during nominal operation, and would only marginally affect the LCOH provided systems run almost continuously. This last condition would specially apply to high CAPEX & low OPEX systems such as high temperature electrolyzers.

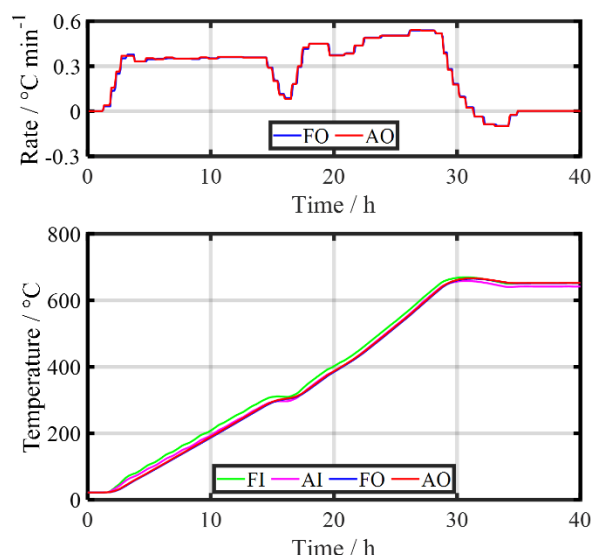


Figure 2: First temperature ramp up of S1 on the durability test bench (FI: fuel inlet, AI: air inlet, FO: fuel outlet, AO: air outlet)

S1 was operated at a constant current density of -0.65 A.cm⁻², chosen to allow comparison with a previous test on a smaller stack [3], and amounting to a stack power of 12.6 kW_{DC}. The evolution of outlet gas temperatures and power over the 3.1 kh durability test is given in Figure 3.

Fuel and air outlet temperatures were recorded near identical over the complete test sequence. Consequently, these measurements are assumed to be a fair estimation of the actual stack temperature. It was about 740°C initially, before increasing linearly at a rate of +15 K.kh⁻¹. Akin to a degradation rate, this result is proficient for assessing the stack lifetime, provided an end-of-life or maximum temperature can be defined. The result is comparable

to what was previously recorded on a smaller stack over the 5-to-7 kh test period ($+12.4 \text{ K.kh}^{-1}$ [3]). It should be noted that this stack had been somewhat extensively performance tested on the production bench, and has spent 700 h in temperature prior to this durability test. Due to the operation strategy, H_2 production (i.e. stack current) and electrical cost (i.e. stack voltage) remained constant throughout the complete sequence [3,15].

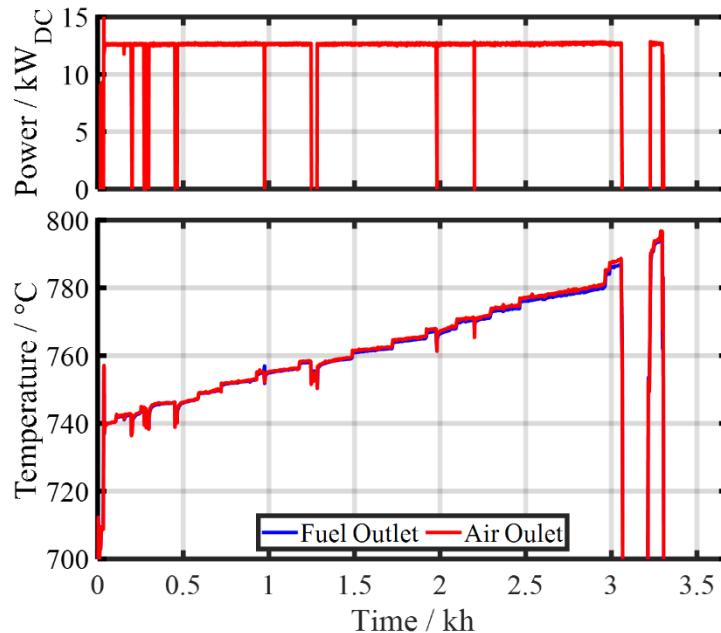


Figure 3 : Evolutions of S1 outlet gas temperatures and power throughout the testing sequence.

After about 3 kh of operation, the stack underwent a thermal cycle for a scheduled bench maintenance. A few days after resuming operation, the voltage of cell n°2, located at the bottom of the stack, suddenly dropped to near 0 V, suggesting a clear cell break. This started a chain reaction that propagated to the 11 bottom cells until combustion could seemingly be mitigated by switching the air side to N_2 . After cooling down the bench, electrical measurements at room temperature highlighted a short-circuit across the corresponding cells. To some extent, the interpretation of test data recorded during the dramatic end-of-life of S1 was confirmed by post-mortem observations following stack disassembly. As shown in Figure 4, a crater spanning the entire 11 cells, larger on repeating unit (RU) n°2 and located at the fuel inlet was evidenced. In addition, strong signs of delamination on most RUs were observed.

Analysis of data tracked throughout the stack manufacturing process highlighted a glass-ceramic thickness for RU n°2 significantly out of tolerance. This would have led to increased mechanical stresses for the cell in operation and at this point is considered the main cause for the stack early end-of-life.

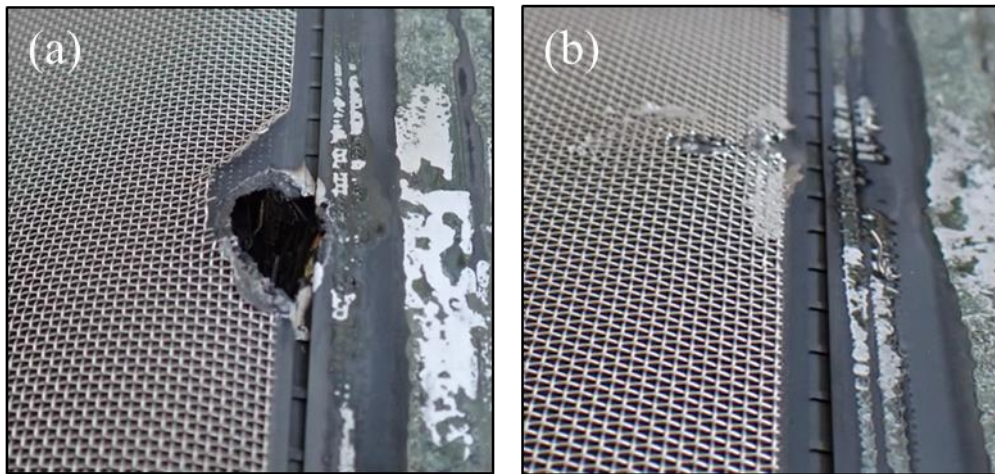


Figure 4: Post-mortem observations of S1: (a) Repeating unit – RU – n°2, (b) RU n°11. Internal leak at the fuel inlet led to various stages of melted interconnects.

2.2. Operation of S2

Following the testing of S1, the components of S2 were manufactured. The stack was then assembled, conditioned (glass-ceramic seal formation and cermet reduction), and performance tested on a production bench. Subsequently, it was cooled down, transported and mounted on the durability test bench.

Due to the much improved stack performances compared to S1, the current density selected for the durability test was increased to -0.94 A.cm^{-2} (-185 A). This set point was a consequence of the steam generator, only able to supply 8.1 kg.h^{-1} (60% SC). The resulting stack power was $18.6 \text{ kW}_{\text{DC}}$. The evolution of outlet gas temperatures and power over the 5.9 kh durability test is given in Figure 5.

Between 0.7 and 1.3 kh, several minor failures of infrastructure networks led to temporary return to OCV, and in one instance, a transition from nominal operation to N_2/H_2 safety gas. At 3.2 kh, before the week-long annual closing of the laboratory, and because of a suspected small internal leak, the inlet air was replaced by N_2 . The resulting lower OCV led to a temporary drop in voltage, which in turn yielded a drop in temperature. From 3.5 kh onward, increasing levels of fluctuations were recorded on the outlet temperatures. This was likely the result of the gas connecting plate, slightly warped at the beginning of the test, deforming further to the point of a leak appearing. Indeed, signs of combustion near the outlet air were discovered on the plate upon unmounting the stack from the bench at the end of the test, corroborating further the slight elevation of temperature recorded by a terminal plate thermocouple located in close proximity. At 4.4 kh, a temporary drop of the deionized network pressure triggered return to OCV and a switch from nominal gas flow to safety gas. While this should not have been problematic, this series of events visibly damaged the tightness level of 3 cells. Indeed, their respective voltage started to plunge. At 5.9 kh, one of these cells broke, triggering the end of the test. This particular cell was notably one of two that showed lower initial performance. At the time of writing, stack disassembly and sample collection for post-mortem analyses have yet to be done.

Over the first 800 h, stack temperature evolved rapidly, from about 735°C to 755°C . This general behaviour has previously been observed [3], and is consistent with several literature reports [13,17]. It was recorded on S2 only because both S1 and S2 were performance

tested over very different durations prior to the start of the durability test: 700 h for S1, and only 200 h for S2. Following this transient start, stack temperature evolved linearly. From 1.0 to 3.2 kh, stack temperature evolved at a rate of $+0.92 \text{ K.kh}^{-1}$. That rate increased to $+1.66 \text{ K.kh}^{-1}$ from 3.2 to 5.8 kh. Given the identical nature of the cells comprising both stacks, this remarkable improvement in cell stability is assumed to be attributed to the stack design modifications implemented on S2 compared to S1.

Interestingly, while S2 was in nominal operation, the total AC-to- H_2 efficiency of the complete test bench, and including electrical steam generation, was $58\%_{\text{LHV}}$. Indeed, power consumption, monitored at all time, was $31.0 \text{ kW}_{\text{AC}}$, with $0.54 \text{ kg.h}^{-1} \text{ H}_2$ being produced (assuming 33.3 kWh.kg^{-1} for the LHV of H_2). Such efficiency, quite high for a single stack test bench, is particularly valuable when testing power stacks due to the energy costs alone.

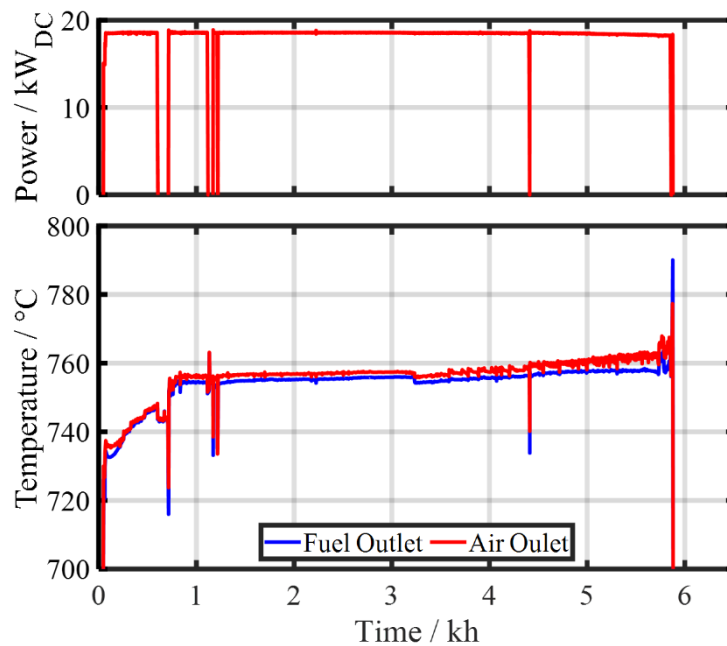


Figure 5: Evolutions of S2 outlet gas temperatures and power throughout the testing sequence.

2.3. Stacks Comparison

Although both stacks comprised a very similar number of cells (75 vs. 78 for S1 and S2, respectively), S2 could be operated at about $+48\%$ power while keeping the temperature at the start of the durability test near identical (740°C vs. 735°C). In addition to the manufacturing success of S2, the results thus highlight a significant boost in performance and H_2 production capacity, achieved while keeping the overall stack component costs stable. Furthermore, during stabilized operation, the two stacks behaved very differently. S1 temperature evolution rate of $+15 \text{ K.kh}^{-1}$ was much higher than S2 (below $+1.6 \text{ K.kh}^{-1}$) in spite of a lower current density (-0.65 A.cm^{-2} and -0.94 A.cm^{-2} , respectively). The cells and interconnect material being identical, these results suggest the design of S1 was largely responsible for its rapid degradation. The different temperature evolution rates suggest the theoretical lifetime at iso-performances of S2, extrapolated up to a maximum acceptable temperature of 850°C , would have been orders of magnitude higher than S1.

Overall, the operation of S1 generated 1.1 ton of H₂ over 3.1 kh, and S2 generated more than 3 ton of H₂ over 5.9 kh. Each of these results constituted back-to-back important internal milestones, and could very well be records of H₂ total production by single stacks in the literature.

With an average cell OCV of 1.157 V ($\sigma = 0.030$ V) in 6 NmL.min⁻¹.cm⁻² of 90/10 vol.% N₂/H₂ and air at 735°C, the initial tightness of the H₂ compartment of S2 was quite good. No major tightness defect could then be detected. The cell breakage in S2 after 5.9 kh of operation could therefore either be the consequence of the geometrical design weakening over time, or the result of a manufacturing defect. Weak spot identification will be one of the main objectives of the upcoming post-mortem observations and analyses. Nevertheless, these results underline the importance of long-term full scale testing to both assess lifetimes and validate designs over technologically relevant durations.

2.4. Test Bench Availability

A preliminary analysis of uptime and “Mean Time Between Failures” (MTBF) recorded in 2023 was carried out to compare three in-house durability benches to commercial testing equipment acquired in recent years from two suppliers. Uptime is defined as the ratio between the time the equipment was either in nominal operation or ready to operate, over the total investigated duration. The annual (and scheduled) technical shutdown of the building lasted 4 weeks in 2023. Because most benches underwent some form of maintenance during that time, it has been considered as (scheduled) downtime. As a consequence, 92% is the maximum achievable uptime. For MTBF calculations (i.e. total hours of uptime / total number of failures), failures are defined as scheduled or unscheduled shutdowns of the bench for repairs and/or modifications. Results, presented in Table 1, have been prepared with a weekly resolution.

Bench	In-house			Manufacturer 1 (M1)			Manufacturer 2 (M2)	
	3 [this work]	2 [15]	1 [18]	M1-3	M1-2	M1-1	M2-2	M2-1
Construction/delivery	2022	2018	2010	2021	2020	2019	2021	2020
Uptime	69%	92%	85%	27%	50%	83%	38%	83%
Average uptime	82%			53%			61%	
MTBF / kh	6.1	N/A ^(a)	7.4	0.8	0.6	3.6	1.1	3.6
Average MTBF / kh	> 7.0			1.7			2.4	

Table 1 : Uptimes and MTBF recorded in 2023 for in-house and commercial benches.

^(a) No failures recorded.

The availability results related to the test bench described in paragraph 1.3 suffered in 2023 from having to replace the stack compression system. This operation took place in between the two test sequences presented in this work. Bench reliability data is expected to become in line with the rest of in-house benches from then on.

Comparing in-house to commercial benches highlights significant differences (Table 1). On the one hand, uptimes are on average much higher, even if some individual results are comparable. Uptimes have a tendency to increase over time, following corrections of infantile issues. However, the period required to improve the robustness of benches varies from about one year in-house, to 3-4 years with commercial equipment. On the other hand, MTBF are strikingly higher in-house. Having reliable benches is particularly crucial with solid oxide technology, as high temperature stacks typically remain fragile to environment failures.

While the results of Table 1 highlight the laboratory's definite competence in producing reliable testing equipment, explaining the difference with commercial benches is more subject to interpretation. Reaching high uptimes require getting a bench back in operation quickly after a failure. However, the process surely will take more time when having to go through multiple echelons of after sale service. Nevertheless, we believe that owning the programmable logic controller (PLC) code, and being able to quickly modify it even while the bench is running, is a core necessity when targeting high reliability. It allows being highly reactive from the early onset of a potential problem, often circumventing it before failures can occur.

Conclusions

Through ongoing efforts to upscale its base stack design, CEA Liten has made two full-scale manufacturing attempts at producing power stacks in the 10-to-20 kW_{DC} range. These stacks, S1, and S2, were tested in this work. S1 was operated for 3.1 kh at 12.6 kW_{DC} and 60% SC up to a cell breakage believed to be a consequence of a manufacturing error. The subsequent manufacturing of S2 yielded a 25% increase in compactness, and an 80% reduction of manufacturing time. The stack could then be operated at 18.6 kW_{DC} for 5.9 kh, up to a cell breakage. The cell breakage that precipitated the end of the test was one of two that showed poor performance from the start of the test sequence. The 1.1 and 3.0 ton H₂ produced by S1 and S2, respectively, constitute consecutive internal milestones and possibly records in the published literature for single stack total production.

These results highlight remarkable progress in stack manufacturing over a short amount of time. Indeed, stack unit power in long-term testing went from 2.1-2.7 kW [3] in 2021, to 12.6 kW in 2022, to 18.6 kW in 2023. The testing of S2 underlines the importance of long-term full scale testing to both assess lifetimes and validate designs over technologically relevant durations.

The type of durability data gathered in this work can only be recorded on reliable benches. The preliminary uptime and MTBF analysis highlighted the laboratory's definite competence in producing reliable testing equipment, particularly when compared to commercial equivalents.

Acknowledgment

This project has received funding from CEA, Genvia, and the Fuel Cells and Hydrogen 2 Joint Undertaking (now Clean Hydrogen Partnership) under grant agreement No 875123. This Joint Undertaking receives support from the European Union's Horizon 2020 research and innovation programme, Hydrogen Europe and Hydrogen Europe research.

References

- [1] Di Iorio S, Monnet T, Palcoux G, Ceruti L, Mougín J. Solid oxide electrolysis stack development and upscaling. *Fuel Cells* 2023;1–8. doi:10.1002/face.202300056.
- [2] Mougín J, Laurencin J, Vulliet J, Petitjean M, Grindler E, Di Iorio S, et al. Recent Highlights on Solid Oxide Cells, Stacks and Modules Developments at CEA. *ECS Trans* 2023;111:1101–13. doi:10.1149/11106.1101ecst.

- [3] Aicart J, Surrey A, Champelovier L, Henault K, Geipel C, Posdziech O, et al. Benchmark study of performances and durability between different stack technologies for high temperature electrolysis. *Fuel Cells* 2023;23:463–73. doi:10.1002/fuce.202300028.
- [4] Aicart J, Tallobre L, Surrey A, Reynaud D, Mougín J. Experimental Report on Galvanostatic Operation of Electrolyte-Supported Stacks for High Temperature Electrolysis. 15th European SOFC & SOE Forum, vol. A0808, Lucerne, Switzerland: 2022, p. 151–62.
- [5] Schwarze K, Geißler T, Nimtz M, Blumentritt R. Demonstration and scale-up of high-temperature electrolysis systems. *Fuel Cells* 2023:fuce.202300059. doi:10.1002/fuce.202300059.
- [6] Di Iorio S, Monnet T, Palcoux G, Ceruti L, Mougín J. Solid Oxide Electrolysis Stack development and upscaling. 15th European SOFC & SOE Forum, vol. A0904, Lucerne, Switzerland: 2022, p. 1–13.
- [7] Mougín J, Mansuy A, Chatroux A, Gousseau G, Petitjean M, Reytier M, et al. Enhanced Performance and Durability of a High Temperature Steam Electrolysis Stack. *Fuel Cells* 2013;13:623–30. doi:10.1002/fuce.201200199.
- [8] Reytier M, Cren J, Petitjean M, Chatroux A, Gousseau G, Di Iorio S, et al. Development of a Cost-Efficient and Performing High Temperature Steam Electrolysis Stack. *ECS Transactions* 2013;57:3151–60. doi:10.1149/05701.3151ecst.
- [9] Di Iorio S, Petitjean M, Petit J, Chatroux A, Gousseau G, Aicart J, et al. SOE stack activities at CEA. 11th European SOFC & SOE Forum, vol. B1307, Lucerne, Switzerland: 2014, p. 1–8.
- [10] Reytier M, Di Iorio S, Chatroux A, Petitjean M, Cren J, De Saint Jean M, et al. Stack performances in high temperature steam electrolysis and co-electrolysis. *International Journal of Hydrogen Energy* 2015;40:11370–7. doi:10.1016/j.ijhydene.2015.04.085.
- [11] Aicart J, Di Iorio S, Petitjean M, Giroud P, Palcoux G, Mougín J. Transition Cycles during Operation of a Reversible Solid Oxide Electrolyzer/Fuel Cell (rSOC) System. *Fuel Cells* 2019;19:381–8. doi:10.1002/fuce.201800183.
- [12] Cubizolles G, Mougín J, Di Iorio S, Hanoux P, Pylypko S. Stack Optimization and Testing for its Integration in a rSOC-Based Renewable Energy Storage System. *ECS Trans* 2021;103:351–61. doi:10.1149/10301.0351ecst.
- [13] Hauch A, Ploner A, Pylypko S, Cubizolles G, Mougín J. Test and characterization of reversible solid oxide cells and stacks for innovative renewable energy storage. *Fuel Cells* 2021;21:467–76. doi:10.1002/fuce.202100046.
- [14] Aicart J, Wullemin Z, Gervasoni B, Reynaud D, Waeber F, Beetschen C, et al. Performance evaluation of a 4-stack solid oxide module in electrolysis mode. *International Journal of Hydrogen Energy* 2022;47:3568–79. doi:10.1016/j.ijhydene.2021.11.056.
- [15] Aicart J, Tallobre L, Surrey A, Gervasoni B, Geipel C, Fontaine H, et al. Lifespan evaluation of two 30-cell electrolyte-supported stacks for hydrogen production by high temperature electrolysis. *International Journal of Hydrogen Energy* 2024;60:531–9. doi:10.1016/j.ijhydene.2024.02.239.
- [16] Strategic Research and Innovation Agenda 2021 – 2027. Clean Hydrogen Partnership; 2022.
- [17] Yang Y, Tong X, Hauch A, Sun X, Yang Z, Peng S, et al. Study of solid oxide electrolysis cells operated in potentiostatic mode: Effect of operating temperature on durability. *Chemical Engineering Journal* 2021;417:129260. doi:10.1016/j.cej.2021.129260.
- [18] Petitjean M, Reytier M, Chatroux A, Bruguière L, Mansuy A, Sassoulas H, et al. Performance and Durability of High Temperature Steam Electrolysis: From the Single Cell to Short-Stack Scale. *ECS Trans* 2011;35:2905–13. doi:10.1149/1.3570290.